Spectroscopic, Photometric and Radial Velocity Membership Selection of the Young Open Cluster NGC 2264 and Subsequent Classification

Dominic Cave
March 2005

ABSTRACT

The work presented here confirms that the photometric identification of T Tauri stars in NGC2264 presented in Sung et al (1997) [S97] is indeed an accurate method. This method identifies members by their position on a V vs. (V-I) Colour-Magnitude Diagram. Two techniques were used in confirming the accuracy – presence of lithium to confirm T Tauri Star status and radial velocity to confirm that the objects are moving together as a group.

The fraction of Classic T Tauri stars in the region was found to be ≈ 30%. This is at odds with the value of 52% ± 10% found by Haisch et al (2001)[H01] using infrared photometric observations to detect the excess in flux at these wavelengths instead of the method favoured here using the equivalent width of the Hα Balmer line.

REFERENCES

Throughout this piece of work, references are given in [square brackets], refer to section 7 for a complete listing.

TABLE OF CONTENTS

Spectroscopic, Photometric and Radial Velocity Membership Selection of the Young Open Cluster NGC 2264 and Subsequent Classification

1. Introduction

Stars are formed when massive clouds of dust and gas become unstable against a gravitational collapse. In the initial stages the gravitational potential energy of the cloud is partly converted into heat energy, and partly retained as internal energy. When the temperature becomes high enough, the process of thermonuclear fusion begins to generate energy as hydrogen is converted into helium. The radiative pressure produced from the nuclear reactions opposes the collapse. The Sun is currently at this stage where the radiative pressure from the nuclear reactions prevents further gravitational collapse. (It was once believed that the power source of stars was just gravitational collapse, but fossil records showed that the earth was older than the calculated age of the sun using this theory.) Subsequent evolution of stars is another topic of interest in astrophysics, but it will not be discussed here. This study is concerned with the evolution of stars from birth up to their appearance on the main-sequence (i.e. when they commence hydrogen burning).

The mechanism by which this cloud collapses into a cluster of new stars is a major topic of research, and many questions remain unanswered. One example of a gap in out knowledge is that the initial cloud appears to have four to six orders of magnitude too much angular momentum – without somehow shedding this excess stars could never form [L04]. Angular momentum of stars effects the way they accrete material, in that accretion disks are formed. The study of circumstellar disks is another topic of interest as it is from these disks that planets are believed to be formed. Knowledge of the timescale on which disks dissipate is vital if we are to know the likelihood of planet formation – a major step towards being able to make an educated guess on whether we are alone in the universe or if intelligent life is commonplace.

Motivated by these gaps in the knowledge of star formation, star forming regions are subjected to extensive observations. Knowledge of the properties of a range of star forming regions or different ages will allow the creation of a timeline of events leading to the creation of stable, main-sequence stars which support life. The property under investigation in this study is the fraction of stars with circumstellar disks.

The target for observations is the young (2-4 million years old [P00]) open (loosely bound by gravity) cluster NGC2264, at a distance of 760pc [S97] (1pc ≈ 3.2 light years, see appendix VI for more details on distance measurements in astrophysics).

Figure 1.1 - NGC2264 – The Target of the Observations
Image taken from http://www.astro-image.com

This study is divided into two parts. Firstly the members of the cluster must be separated from the foreground and background objects. There are many ways of achieving this, three methods are discussed in section 2.4. We make use of three membership tests so that a robust list of members can be created. Once this has been achieved the fraction of members with disks can be found and compared with previous studies of the region, and also with data from star forming regions of different ages.

2.1. Background Theory I – From the Interstellar Medium to the Main Sequence

The space in between stars is not a perfect vacuum, it is filled with the so-called interstellar medium (ISM), a mixture of gas and dust which pervades our galaxy. The majority of the gas is hydrogen and helium but also present are small amounts of other elements created in the previous generation of stars and ejected in the latter stages of stellar evolution and a small amount of silicate and carbon based grains of dust. The ISM is not uniformly distributed through the galaxy but instead it is clumped into interstellar clouds of various sizes and densities.

Consider one of these clouds of gas, and assume that it has found an equilibrium state of uniform density. The cloud is perturbed (perhaps by a shockwave from a supernova) and part of it is compressed. The gravitational pull from this region of space will increase, tending to attract more mass and thus initiating a gravitational collapse. At the same time however the pressure

of the compressed region has increased which leads to an expansion to counter and smooth out the perturbation. For a gravitational collapse to occur leading to the initiation of star formation, the cloud must contract, and it can be shown that for a given temperature (T) and density (ρ) of the cloud there is a maximum stable mass, the Jeans mass M_J ($M_J \propto \rho^{\frac{-1}{2}} T^{\frac{3}{2}}$) (See Appendix I for derivation). For a dense molecular cloud, the maximum stable mass is around a hundred times the mass of the sun, so there must be some form of fragmentation occurring before the stars are formed. This fragmentation is due to the efficiency of heat transport through the cloud as it collapses. If the heat transfer is isotropic then the heat transfer is effective enough to keep the gas at a constant temperature and M_J decreases as the density increases, meaning smaller masses within the cloud become unstable against collapse. When the cloud can no longer remain isothermal the fragmentation ceases (M_J then increases with density, $M_J \propto \rho^{\frac{1}{2}}$ for an ideal monatomic gas, see appendix I for derivation)

During the collapse, the radius of the cloud decreases by around 10^4 times. Angular momentum conservation leads to the conclusion that angular momentum is an important part of star formation, even if the initial cloud only had a very small rate of rotation. The formation of discs (covered in depth in the next section) is an important result of this rotation.

From this point there are two possibilities – either contraction continues until the temperature becomes high enough to ignite hydrogen burning, or such a temperature is never reached. In the first case, when a temperature of 10 million degrees Kelvin is reached, hydrogen burning commences and the star is born. This is the beginning of the main sequence stage of evolution. (Note, before hydrogen burning is ignited the star can burn other fuels such as deuterium, however the ignition of hydrogen burning is required for the object to be classed as stellar). The latter scenario results in a 'failed star' or 'brown dwarf'. See [K05] for a more detailed account of brown dwarfs, as they will not be mentioned again here.

Young Stellar Objects (YSO) are frequently deeply embedded in the gas clouds from which they formed. In the early stages of life they are only visible through infrared observations. Four classes of YSO are classified –

- Class 0 – Extremely young 'protostars' deeply embedded in molecular cloud.
- Class 1 – Typically around 100,000 years old these objects have accumulated a large fraction of their final mass
- Classes 2 and 3 – T Tauri stars. These stars are now optically visible as they are no longer embedded within molecular clouds.

Observations of the class 2 and 3 objects, although now optically visible, still suffer large extinctions (see section 2.3).

2.2. Background Theory II – Accretion Discs and Classification of T Tauri Stars (Classic and Weak-lined)

There is a distinct class of stars which are typically less than 2 solar masses and younger than 10^6 years. These are named T Tauri stars (TTS) and were originally identified on the basis of their broad (Equivalent Width > 10Å) Hα Balmer emission line (6562.85Å) and infrared excess.

During the process of accretion, the material does not fall from the disk to the star in a straight line, instead is confined to follow the magnetic field lines. The charged particles will spiral around the magnetic field lines as the fall onto the star, resulting in blue and red Doppler shifting of inflowing material and the creation of broad emission lines. As the accreting material is mainly hydrogen this effect is most obvious in the Balmer emission lines, the strongest of which is the aforementioned Hα line. The presence of broad Hα is therefore indicative of ongoing accretion.

The dust in the disk absorbs the photons emitted from the star and re-emits them isotropically toward the infrared end of the spectrum, creating the infrared excess. The presence of an infrared excess is therefore indicative of the existence of circumstellar material.

Young stars are almost entirely convective, which produces strong magnetic fields due to the movement of the charged particles (atoms within stars are ionized due to the high temperatures of ~10^7 K). This creates large magnetic loops on the surface of the star creating flares, and as the plasma is channelled along these field lines the process of bremsstrahlung (braking radiation) results in strong X-ray emission. These effects are seen with reduced strength in the sun (see figure 1.2)

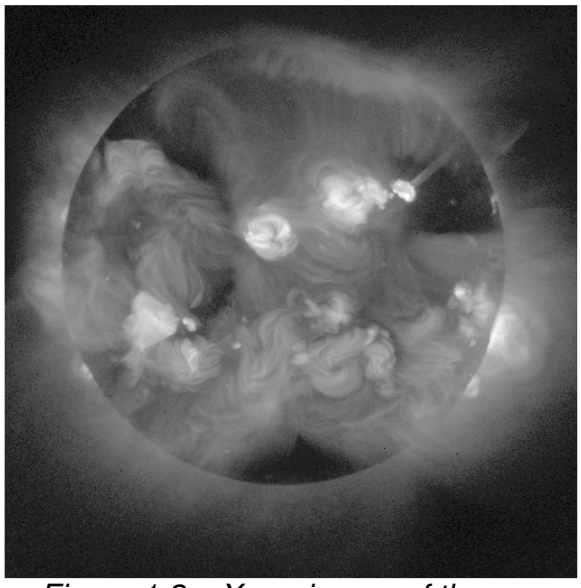

Figure 1.2 – X-ray image of the sun
From the Japanese 'Yuhkoh'(Sunbeam) Observatory [YO]

Stars which exhibit strong X-ray emission but lacked the broad Hα line and infrared excesses were discovered, and became known as 'Weak-lined T Tauri Stars' (WTTS) – i.e. they were TTS but they lacked their circumstellar disk. The stars originally designated as TTS are now known as 'classic TTS' (CTTS). The 'classic-to-weak' ratio is an important characteristic of a star forming region – and comparisons between regions of differing ages will give a very good indication of how quickly the circumstellar disks dissipate. By direct comparison of this timescale with that required for planets to form around a disk we can estimate the fraction of stars which have a planetary system. (This is one of the parameters required for the 'Drake Equation' which estimates the likelihood of intelligent life existing elsewhere in the universe).

The method by which disks are dissipated is also of interest. It is thought that high mass (and therefore high luminosity) stars are responsible for this process – this could be tested by plotting the CTTS, WTTS and high mass stars on a single map and plotting the classic-to-weak ratio as a function of radial distance from the massive stars.(See [S04] for an infrared photometric study of NGC 3603.)

2.3. Background Theory III – Introduction to Photometry

The system used to quantify luminosity in astrophysics is based on the system introduced by the Greek astronomer Hipparchos in around 180 BC. He created an extensive catalogue of stars based on naked eye estimates alone. The adopted system is that the brightest star visible to him would have a magnitude of 1 and the faintest star would have a magnitude of 6. The magnitude 1 stars are ~100 times as bright as the magnitude 6 stars, so if a star is 1 magnitude brighter than another it is ~2.5 times brighter ($2.5^5 = 100$). Note that these measurements describe *apparent* magnitude and are not a measure of the intrinsic luminosity of the star (a brighter star at a greater distance may have the same *apparent* magnitude as a closer but dimmer one).

Stars do not emit photons of different frequency in identical amounts. Hotter stars emit a larger proportion of higher energy photons than cooler stars, and therefore appear bluer (from the Planck relation, $E=h\upsilon$) In order to make these measurements more precise we should define exactly which section of the electromagnetic spectrum we are considering. Table 2.3.1 shows the accepted values of filters used in 'Kron-Cousins UBVRI' photometry.

Filter Pass band	Central Wavelength (nm)	Width at 50% of Peak (nm)
U	367	66
B	436	94
V	545	88
R	638	138
I	797	149

Table 2.3.1 – UBVRI Photometry Filters ([M98] and references therein)

From this information, we can quantify the colour of a star as the difference between two magnitudes. For example, consider a colour (B-R). A blue light source would have a low magnitude (high brightness) when looking through the blue filter and a higher (fainter) magnitude through the red filter. The (B-R) colour would have a negative value. Now consider a green light source, green is midway between blue and red in the electromagnetic spectrum and so the (B-R) colour would be zero. Similarly a red light source would have a positive (B-R) colour.

An important tool in observational astrophysics is the colour-magnitude diagram (CMD). Generally a magnitude is plotted on the vertical axis and a colour on the horizontal axis (see figure 2.3.2)

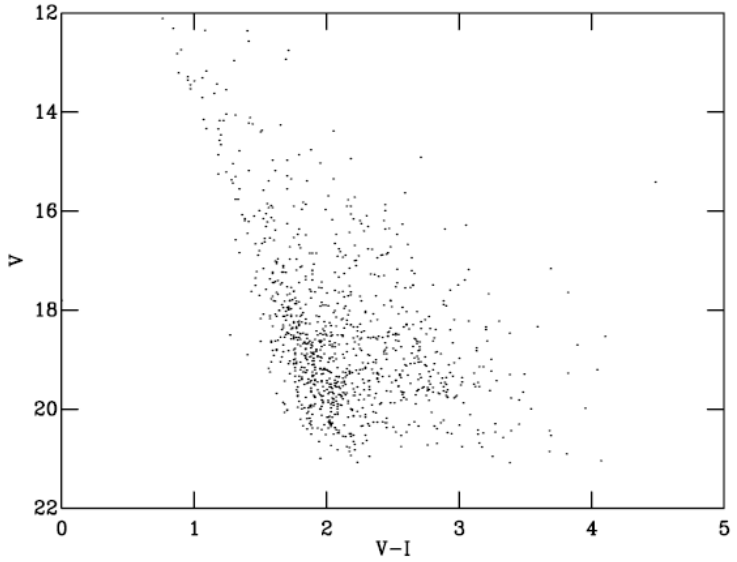

Figure 2.3.2 – Example of a CMD. The brightest stars are higher up on this graph (due to the inverted vertical axis), and the redder stars are further toward the right.

The effect of extinction (dust obscuring the view of a stellar object) is that the star moves down and right on a CMD. The star appears fainter as some of

the incident light as absorbed by the dust and re-emitted in a different direction and it appears redder as the higher energy photons are scattered more strongly than redder ones (the same physical process which explains why the sky is blue during the day and red at sunset and sunrise – see chapter 11.1.2 of [DG] (Electric Dipole Radiation) for a detailed explanation)

2.4. Background Theory IV – Identification of Young Stars (Membership Tests)

Before we can start any kind of analysis on a cluster of stars (in this case NGC2264) we must separate the members of the cluster from the foreground objects. I have considered three methods of membership test – the presence of lithium (via spectroscopic measurements), radial velocity (through Doppler shift measurements) and a 'photometric cut' method.

Photometric Cut Method

In the study presented by Sung et al (1997), henceforth [S97], UBVRI Hα photometry was carried out (i.e. UBVRI photometry as described above but with an additional filter centred on 6563 Å, the wavelength corresponding to the Hα Balmer line). The CMD on the left in figure 2.4.1 shows the stronger Hα sources further to the right. The CMD on the right shows the stars classified as pre-main-sequence (PMS) in a V vs. (V- I) plot, showing the PMS objects in the region of the CMD expected for objects in a very dusty environment (due to the effects of extinction).

The validity of this type of selection will be evaluated through comparisons with spectroscopic data as part of this study.

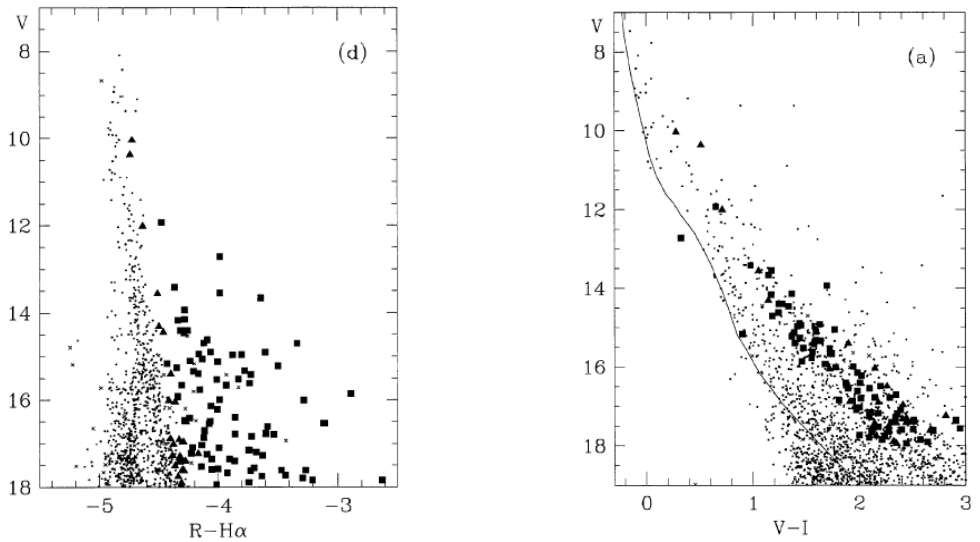

Fig 2.4.1 – CMDs taken from [S97]. The filled in squares and triangles indicate pre-main-sequence objects

Spectroscopic Method – the Lithium Criterion

Lithium is never produced in the thermonuclear reactions within a star, and any which is present is quickly depleted once thermonuclear reactions commence. Due to the convective nature of young stars, lithium from any part of the star is quickly transported to the core of the star (where the temperature is high enough for the thermonuclear reactions to take place) and depleted. As any main sequence star destroys the lithium quickly, the presence of Lithium in a star implies that is a pre-main-sequence object.

The lithium doublet (6707Å & 6709 Å) will always appear as an absorption line in the spectra due to the fact that we only see the photosphere (surface) of the star and the photons from the centre of the star are absorbed by the lithium, and subsequently emitted isotropically. This means that the amount of emission is dwarfed by the amount of absorption. The doublet will appear as a single line as they are very close to each other and errors in the measurement and limitations on the resolution of the spectrograph will blur out any double-lined feature.

Figure 2.4.2 shows an example of one of the WTTS identified using this method.

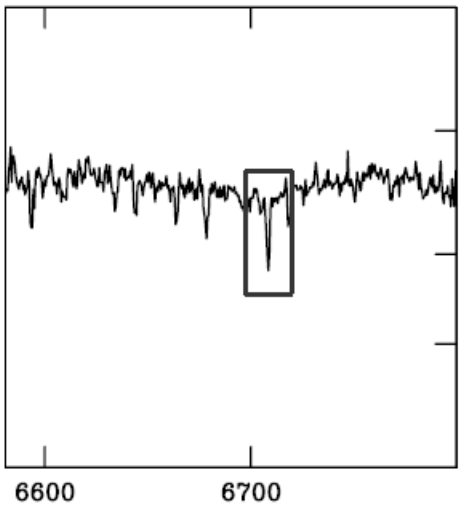

2.4.2- Example of a strong lithium absorption line

The accepted lithium criterion is that the equivalent width of the lithium should be greater that 200mÅ. In figure 2.4.3, the area under the dotted line is the same in both graphs – by changing the shape of the absorption line into a rectangle of a known height we can calculate the 'equivalent' width, measure in the same units as the wavelength.

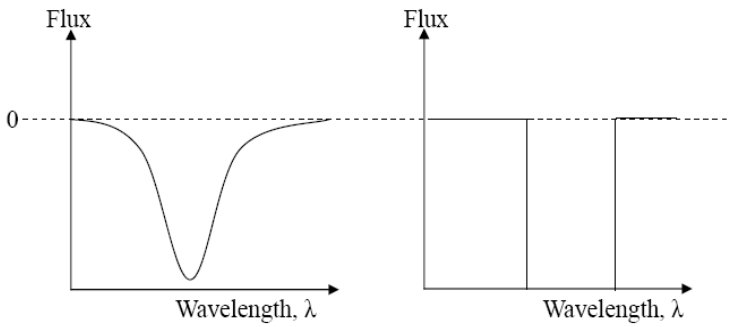

2.4.3 – Equivalent Widths. The dotted horizontal line represents the continuum level.

The equivalent width measurement is used as it is independent of observation exposure time. If the spectrograph is exposed to the light for longer, the line will be more pronounced, increasing the area under the continuum band. At the same time the height of the continuum band increases, but the equivalent width measurement remains unchanged. This is obviously an important feature of equivalent widths as it allows comparisons with other observations taken under different conditions.

Radial Velocity Method

Velocities of individual stars can be expressed as two components – the velocity along the line of sight (i.e. the velocity either towards or away from the earth) and the velocity tangential to this line of sight. Velocities tangential to our line of sight require more than one set of observations, but we can use the *radial* velocity to select members of a cluster, which will obviously be all moving with the same velocities.

Radial velocities can be derived from spectroscopic data by considering the relative Doppler shift of the absorption/emission lines. By considering one reference star, we can compare the wavelengths of certain absorption lines with wavelengths of the same lines in the other stars in our spectroscopic catalogue to get a radial velocity measurement.

There are effects which would complicate this simplistic picture where all members of the cluster move with identical velocities. Binary and higher order systems of stars within the cluster, together with any rotation or expansion of the cluster as a whole will cause a spread in radial velocity measurements. A radial velocity spread of ~10-12 km s^{-1} around an average value is common.

Reliability of Membership Tests

The reader may have doubts about some aspects of what is described here, for example - a foreground object which is close enough to the cluster in question to give a radial velocity within the spread of velocities allowed for membership will be wrongly classified as a member. The name has been carefully chosen to imply that the classifications are far from infallible. For an

object to be confidently classified as a pre-main-sequence object it must pass a number of these membership tests.

3. Observations – Photometric and Spectroscopic Data Acquisition

The photometric observations were taken using the wide field camera (WFC) at the 2.5m Isaac Newton Telescope (INT) and the spectroscopic observations were taken using AF2/WYFFOS multi-object, wide field fibre spectrograph at the 4.2m William Herschel Telescope (WHT) at the Isaac Newton Group of telescopes on La Palma [ING].

Fibre Spectroscopy

The major disadvantage of spectroscopic observations is the fact that only one object can be analysed at a time. Given the relatively long exposure time required for spectroscopic observations to achieve a high signal to noise ratio this ends up to be costly. Fibre spectroscopy offers a solution to this problem by allowing 150 observations to be taken in one go. As the name suggests, the solution is to use lengths fibre optic material to in effect separate out the light from each object. A robot is used to position the fibres in the correct place to speed up the process and ensure accuracy.

The Spectroscopic Data

In each file containing the data for a spectrum there should be information on where the star is in the sky, what the target for the spectrum was (i.e. object or sky) and the magnitude of the object. Half of the data available for this investigation was unfortunately lacking in this information. It will be made clear in this report when only half of the data available is being used.

4. Handling the Data – Sky Subtraction of Spectra and Reduction of Photometry

Sky Subtraction of Spectra

Earth based spectroscopic observations of the of stars are unavoidably contaminated by the spectrum of the night sky, so during the observations additional measurements are taken which are intentionally placed to avoid having a star in the line of sight. These sky spectra can then be subtracted from the data received from observations of stars to leave a reliable set of spectra to work with.

There is one other consideration – that of ‘cosmic rays’ (any particle that comes from beyond the earths atmosphere is termed a cosmic ray). If a single high energy particle were to strike the telescope during an observation it will be significant. To resolve this problem we take multiple sky spectra an

median stack them (i.e. for each wavelength step take the middle value of the flux of each of the inputs). This method works as in general we take 5 sky spectra, so unless 3 of them have a cosmic ray at a particular wavelength (extremely unlikely!) we will effectively remove the problem (as an aside it is worth noting that taking the average would only serve to limit the problem rather than eradicating it).

All sky spectra are similar, however the process must be carried on each night as local effects as well small variations in the composition of the atmosphere can also significant.

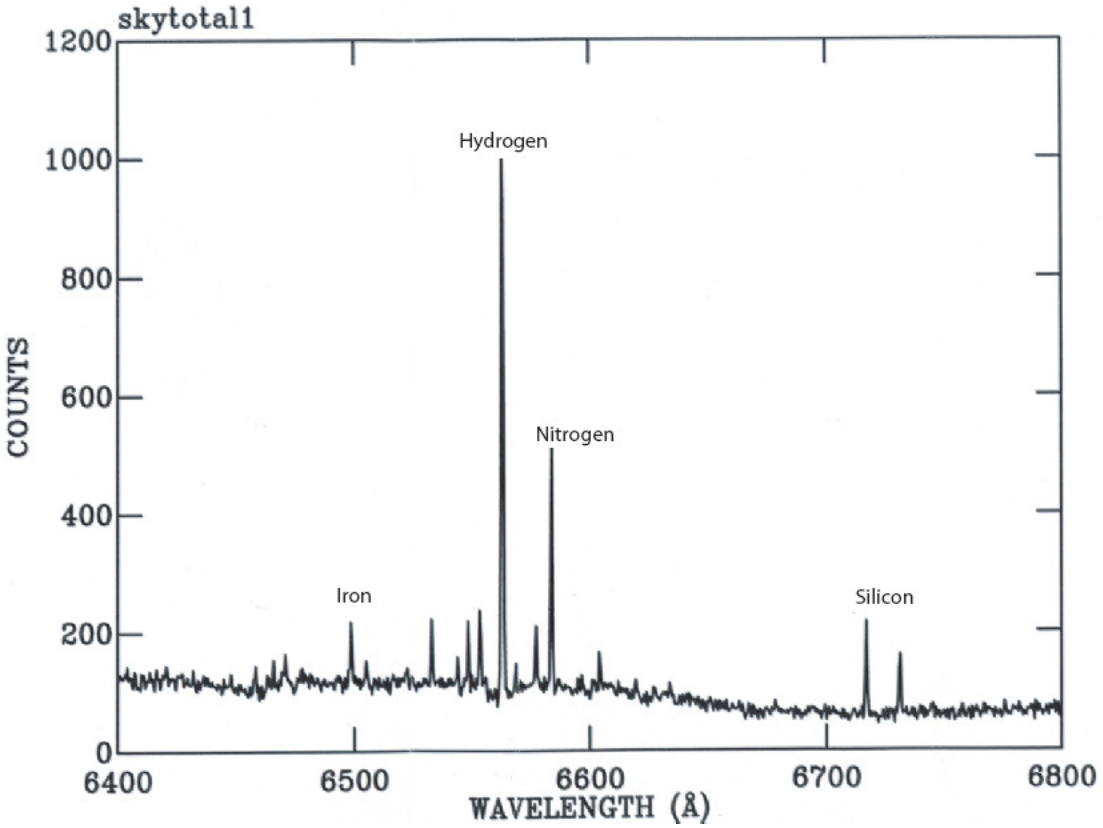

Figure 4.1- Example of a Sky Spectrum, with strong emission lines marked

Reduction of Photometry

Due to the large area for which coverage is required, four separate observations were required. Each of the four regions were reduced separately and then combined to form a mosaic image (on figure 4.2 the separate CCD images are distinguishable)

The data from the telescope comes in the form of an image as recorded by the CCD (or in the case of the Isaac Newton Telescope, 4 CCDs). A short (2s) and long (20s) image is taken for each region of the sky required. The 20s exposure detects stars down to 20th magnitude in the V band, whereas the 2s exposure is used for photometry on the brighter stars in the region, those which are saturated on the long exposure.

Charged couple device (CCD) cameras are made up of individual pixels, each varying in their sensitivity to light and heat. Ideally all of the pixels would be equally sensitive to light and not effected by heat at all. The temperature of the CCD camera is kept as low as possible but any temperature above absolute zero will create what is known as a dark current. The amount of dark current can be calculated by taking a picture in complete darkness and the variance of the sensitivity of each pixel to light can be calculated by a process known as flat fielding (using a homogeneously illuminated image).

The positions of the objects on the CCD are extracted first, and then the photometry is carried out on each of the detected objects. Converting the positions on the CCD into real RA and Dec (right ascension and declination) requires external catalogues of bright stars, for example the '2 micron all sky survey' (2mass) [2MA]. This is obviously not in any way a complete description of the process, but the detailed procedure is beyond the scope of this study.

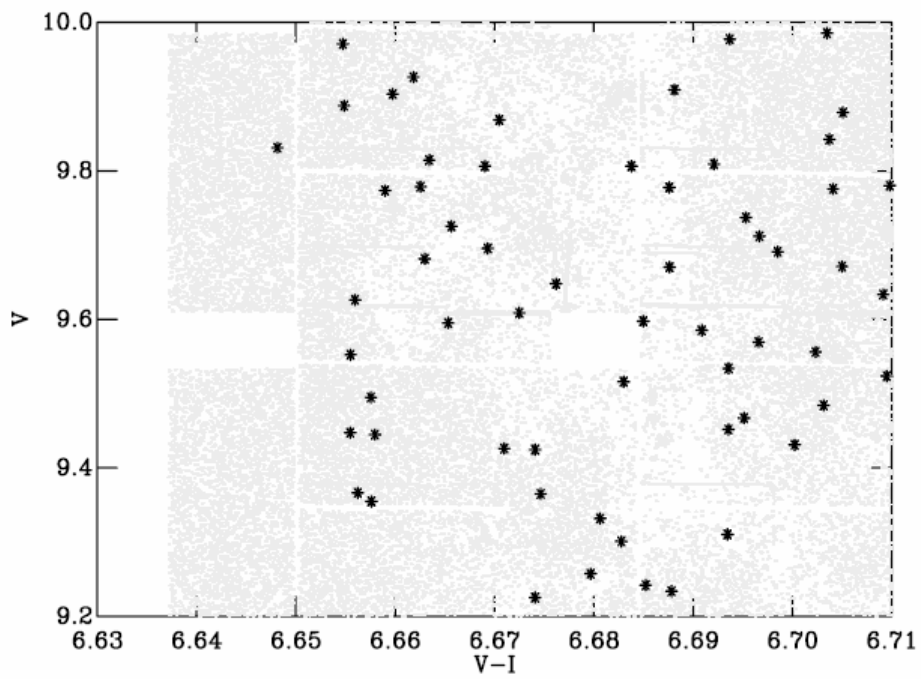

Figure 4.2 – Map of NGC2264, the asterisks mark stars for which we have spectroscopic data.

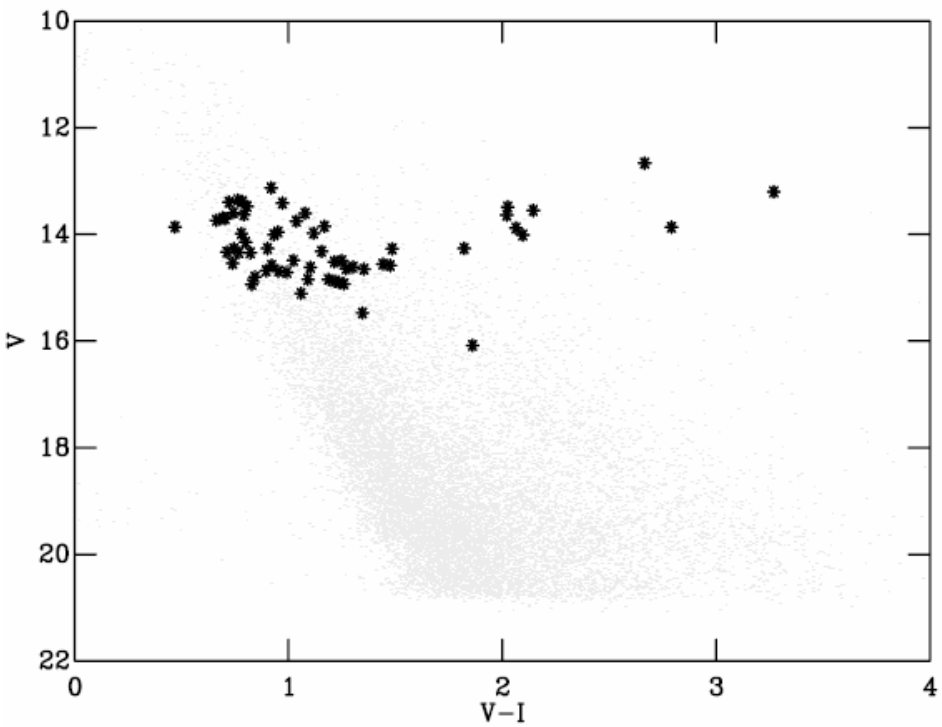

Figure 4.3 – CMD of NGC2264, again with asterisks marking stars for which spectroscopic data is available

5. Results

Errors in Photon Counts

To estimate the error in a calculation involving counting photons we recognise that the distribution of photons follows a Gaussian distribution about an average value (i.e. the photons arrive randomly but with a mean number per second on N) –

$$p(n) = \frac{1}{\sqrt{2\pi N}} e^{-\frac{(n-N)^2}{2N}}$$

In a distribution of this type, there is a 67% chance that the number of photons counted will be $N \pm \sqrt{N}$. The value $\sqrt{N}$ is therefore the associated error in the measurement.

Membership Test 1 – Presence of Lithium in Spectroscopic Data

Equivalent width measurements were made for each object with spectroscopic data in a fully automated process, with visual checks made before any object was classed as a T Tauri star. Anomalies such as cosmic rays can fool the automated process into thinking lithium is present when in fact it is not. (The line that is supposed to be representing the continuum is

too high, creating an area of the line that is too large which manifests itself in a large equivalent width). The automated process provides an equivalent width for lithium, EW(Li) and an associated error, EWerr(Li). By starting with the objects where EW(Li) – 2EWerr(Li) > 200mÅ (i.e. even if the error is taken off twice it still qualifies as TTS) and working down until there is no sign of lithium in the spectra we find the limit of acceptability, the point at which the object cannot confidently be classified as TTS.

The calculated equivalent width should be significantly greater than the error for any result to be taken with confidence, and by introducing the criterion that $\frac{EW(Li)}{EWerr(Li)} > 1.5$ successfully reduced the number of spurious results attained from the process.

This process identified 14 T Tauri stars (See appendix VII for the spectra).

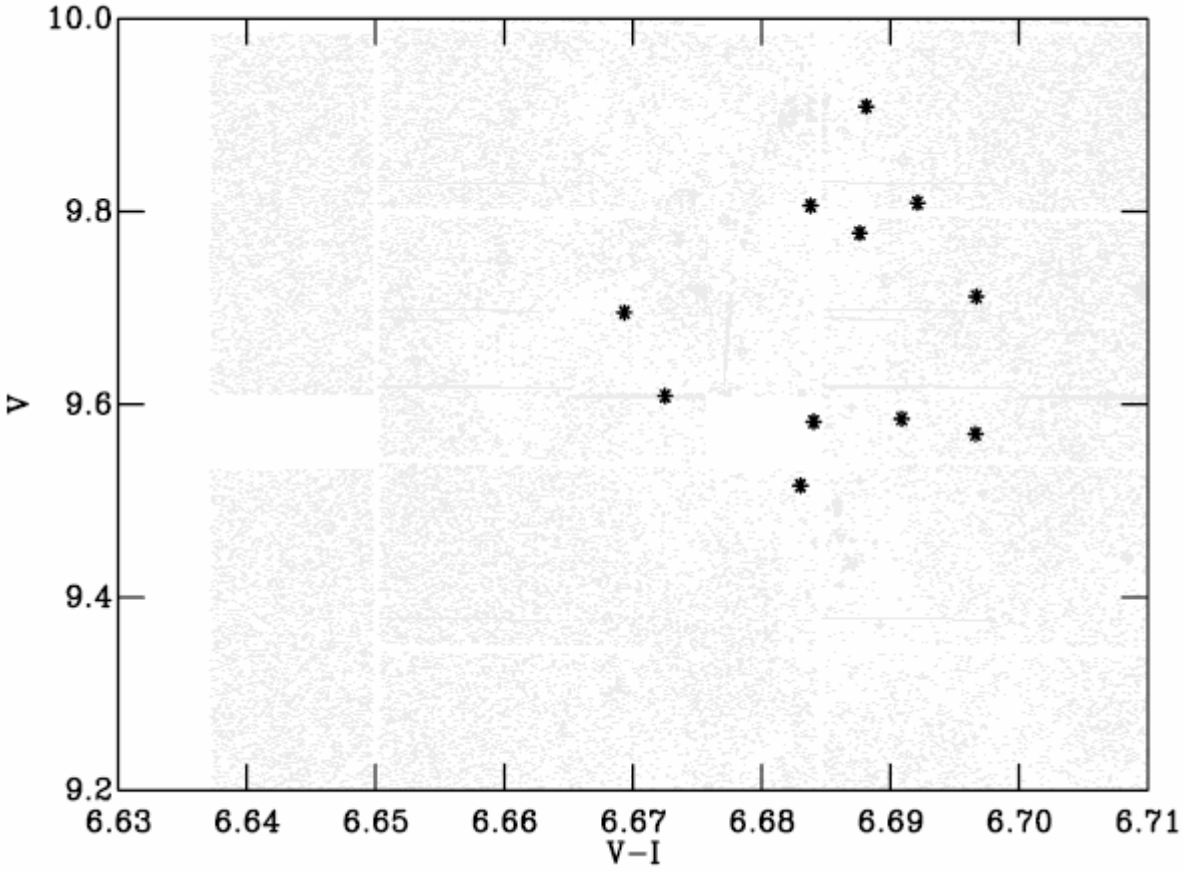

Figure 5.1 – The TTS marked on a background map of NGC2264
Comparison with [S97] – Critical Evaluation of the Photometric Cut Method

For this test, only half of the spectra are available (see section 3). Fortunately, most of the T Tauri stars identified are included in the useful spectra (11 of the 14). By cross-correlating with our photometric catalogue we find counterparts to 10 TTS (One is in a small region in the centre which is not covered). An additional T Tauri star is lost as it unfortunately falls on a row of bad pixels on the CCD. As figure 5.1 shows , the 9 TTS fall in the correct place in the CMD – providing evidence to support the photometric cut method of TTS selection used in [S97].

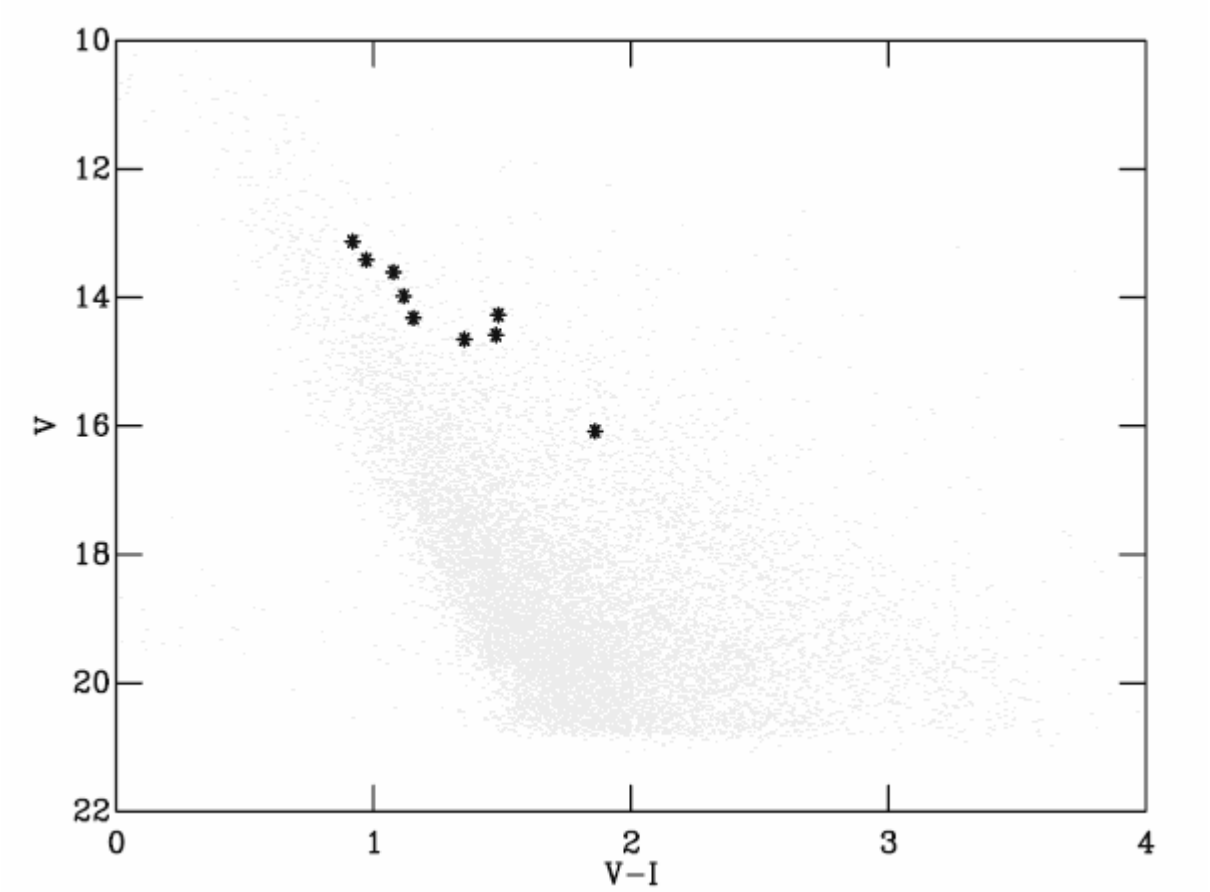

Fig 5.2 - CMD Supporting Photometric Cut method used in [S97]
(for comparison, see figure 2.4.1)

Membership Test 2 – Radial Velocity Measurements

The reference star chosen for this measurement is a not a member of NGC2264 to ensure a independent evaluation. Figure 5.3 shows a band of TTS between a relative radial velocity of 10kms^{-1} and 40kms^{-1}, which implies a spread of 15kms^{-1} around the average value. This result is expected as it is very unlikely that any foreground objects are also TTS, it is however a valuable result in that it supports the conclusions drawn so far.

The reader will notice that there are some stars within the band of TTS which have not been selected as members. This is expected as some of the stars

may be at the same distance from the earth but not at the same coordinates as NGC2264 (see figure 4.2 for a map of the observations.)

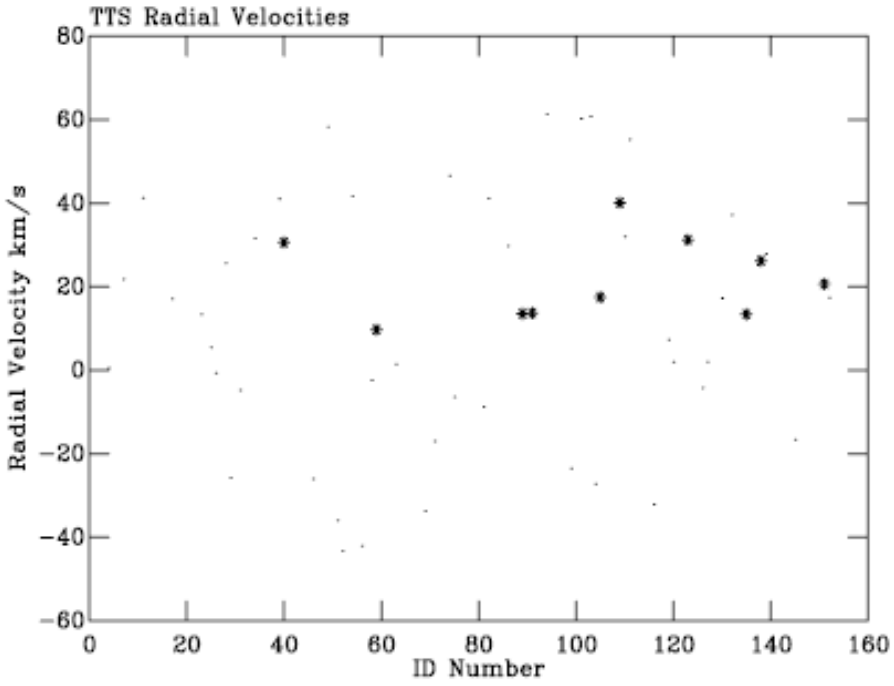

Figure 5.3 – The dots represent the radial velocities of all the stars, whereas the stars represent the TTS

The Classic-to-Weak Ratio – f (CTTS)

Using the 14 TTS identified on the basis of their lithium content by the spectroscopic observations, we run a similar technique to ascertain the equivalent width of the Hα Balmer line. The definition of a CTTS (Classic T Tauri Star) is that EW(Hα) > 10Å. On this basis there are 4 CTTS and 10 WTTS, giving a disk frequency *f*(CTTS) ≈ 29%. Visually the distinction between CTTS and WTTS is often clear – and this is the case for the 14 TTS presented in Appendix VII.

6. Conclusions

The work presented here first confirmed that the photometric identification of T Tauri stars in NGC2264 presented in Sung et al (1997) [S97] was indeed an accurate method. The TTS all appeared in the band redward of the rest of the stars, without exception. Even taking into consideration the small number of TTS used, the fact that not one of them was out of place inspires confidence in the method.

Radial velocity measurements were carried out, and although they would be of little use without other membership tests they did confirm that the membership list was accurate, and that the spread of radial velocities around the average was 15 kms^{-1}.

The fraction of Classic T Tauri stars in the region was found to be ≈ 29%. This is at odds with the value of 52% ± 10% found by Haisch et al (2001)[H01] using infrared photometric observations to detect the excess in flux at these wavelengths instead of the method favoured here using the equivalent width of the Hα Balmer line. (The current definition of a CTTS is that it has both of these features, see section 2.2)

A possible reason for this discrepancy is the Haisch et al, although working with more TTS than in this investigation, did not cover the whole region, it is specifically targeted toward the southernmost section – whereas this investigation covers the whole region. It is quite acceptable to conclude that the region Haisch covered is more densely populated by disked TTS. An attempt was made to plot the classic and weak lined TTS on a map of the region but using only 2 CTTS and 9 WTTS it was difficult to confidently predict anything.

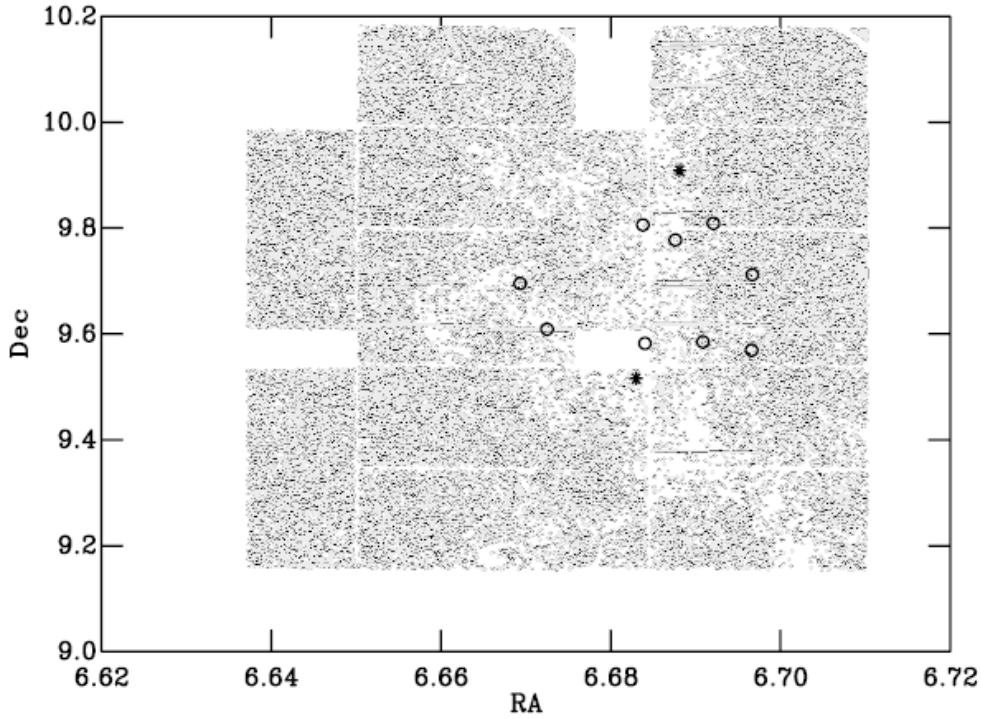

Figure 6.1 – CTTS (asterisks) and WTTS (circles) plotted on a map of the region.

It is worth considering the other interpretation of the results. Assuming now that both the work presented here and that of Haisch et al are representative of the whole cluster, we can work backwards and conclude that it is not right to group TTS into those with broad emission lines *and* infrared excesses and those that lack both features. The broad Hα lines used in this work are indicative of accretion whereas the infrared excesses are indicative of the presence of a disk. Perhaps some TTS are stable disked systems? This is merely speculation and more observations would be required to justify the suggestion. A spectroscopic study aimed specifically at the TTS in the catalogue presented by Haisch et al would be able to answer the question of whether or not the CTTS identified on the merit of IR excess did indeed all also have broad Hα lines.

Another area of study is the effect of high mass stars on low mass star formation (see [MPT]). The massive star S Mon is positioned very close to the upper CTTS in figure 6.1, despite the fact that high mass stars exit a stellar wind of particles at very high velocities which should easily strip any low mass star of its disk. With only 2 CTTS for which the positions are known (due to problems with one half of the data), it is impossible to say whether or not this is a one off or a common feature. With more data a pattern may arise and it is likely that CTTS close to massive stars is a rare observation. An infrared photometric study of the NGC 3603 region presented in Stolte et al (2004) [S04] indicates a radial increase in f(CTTS) from 20% to 40% from the core to the cluster outskirts. It would make sense if this was a typical observation.

7. References

*Links to the World Wide Web are correct as of March 2005, but may change at any time.

[2MA] – 2 micron all sky survey - http://www.ipac.caltech.edu/2mass/
[ADS] – NASA Astrophysics Data System - http://adswww.harvard.edu/
[CDS] – CDS services, University of Strasbourg
http://cdsweb.ustrasbg.fr/CDS.html
[DG] – Introduction to Electrodynamics Third Edition, Griffiths, DJ, Prentice Hall (1999)
[H01] – Disk Frequencies and lifetimes in young clusters, Haisch and Lada, The Astrophysical Journal, 553:L153-L156 (2001)
[ING] – Isaac Newton Group of Telescopes - http://www.ing.iac.es/
[K05] – Kendall et al 2005 - A deep, wide-field search for substellar members in NGC 2264 (from arXiv preprints archive - http://www.arxiv.org/)
[L04] – A rotational and variability study of a large sample of PMS stars in NGC 2264, Lamm, MH, Astronomy and Astrophysics, v.417, p.557-581 (2004)
[M98] – UBVRI photometry using CCD cameras, Richard Miles, J.Br.Astron.Assoc 108 p 65-74 (1998)
[MPT] – The effect of high mass stars on low mass star formation, M Pozzo, 2001. (PhD Thesis)
[P00] – The Pre-Main-Sequence Stars and Initial Mass Function of NGC 2264, Park, B - The Astronomical Journal, Volume 120, Issue 2, pp. 894-908. (2000)
[S97] – UBVRI H(alpha) Photometry of the Young Open Cluster NGC 2264 Sung,H, Astronomical Journal v.114, p.2644 (1997)
[S04] – The Secrets of the Nearest Starburst Cluster. I. Very Large Telescope/ISAAC Photometry of NGC 3603, Stolte, A The Astronomical Journal, Volume 128, Issue 2, pp. 765-786 (2004)
[YO] – Yuhkoh Solar Observatory (Japanese Satellite)
http://www.lmsal.com/SXT/
[UEA] – University of Exeter Astrophysics Group http://www.astro.ex.ac.uk

8. Appendices

I DERIVATION OF THE JEANS MASS

If the cloud is in virial equilibrium (i.e. the total internal energy of the cloud is equal to half of the gravitational potential)

$$E = \frac{1}{2}\Omega$$

The total energy is equal to the sum of the sum of the kinetic and potential energy

$$\Omega + K = \frac{1}{2}\Omega$$
$$\Omega + 2K = 0$$

Consider a spherical cloud of uniform density ρ with N particles at a temperature of T

$$K = \frac{3}{2}Nk_BT$$

Where k_B is Boltzmanns Constant

The gravitational potential of a uniform sphere is

$$\Omega = -\frac{3}{5}\frac{GM^2}{R}$$

Where G is the gravitational constant, M is the mass and R is the radius. The virial equation then reads

$$\frac{3}{5}\frac{GM^2}{R} = 3Nk_BT$$

If the left hand side of this equation is largest, the cloud will contract under gravity.

If we introduce the mean molecular mass μ and the mass of a hydrogen molecule m_H such that

$$N = \frac{M}{\mu m_H}$$

The density is simply represented by

$$\rho = \frac{M}{\frac{4}{3}\pi R^3}$$

Rearranging this gives

$$R = \left(\frac{3}{4} \frac{M}{\rho \pi} \right)^{\frac{1}{3}}$$

$$GM^2 \left(\frac{4\rho\pi}{3M} \right)^{\frac{1}{3}} = \frac{5Mk_B T}{\mu m_H}$$

Simple rearrangement gives the answer quoted in the section 2.1.

$$M_J = \left(\frac{5k_B T}{G\mu m_H} \right)^{\frac{3}{2}} \left(\frac{3}{4\pi\rho} \right)^{\frac{1}{2}}$$

$$M_J \propto T^{\frac{3}{2}} \rho^{-\frac{1}{2}}$$

And now to consider when the fragmentation process stops, as discussed in section 2.1

In an adiabatic gas (i.e. one that retains its heat rather than efficiently radiated away)

$$pV^{\gamma} = const$$

$$p \propto TV^{-1}$$

$$\therefore$$

$$TV^{\gamma-1} = const$$

Here, γ is the adiabatic index. As $\rho_n V = N$ (where ρ_n is a number density)

$$T \left(\frac{N}{\rho_n} \right)^{\gamma-1} = const$$

$$T \propto \rho_n^{\gamma-1}$$

For an ideal monatomic gas, the adiabatic index is $\frac{5}{3}$, and so the Jeans Mass is

$$M_J \propto T^{\frac{3}{2}} \rho^{-\frac{1}{2}}$$

$$M_J \propto \left(\rho^{\frac{2}{3}} \right)^{\frac{3}{2}} \rho^{-\frac{1}{2}}$$

$$M_J \propto \rho^{\frac{1}{2}}$$

Hence as the density of the cloud increases, the Jeans mass increases too – and so further collapse is no longer possible and the process of fragmentation stops.

II THERMONUCLEAR FUSION

A full treatment of thermonuclear fusion is not given here. What is given is a description of the main process of energy generation is low mass stars, the proton-proton chain.

(key – proton (p), positron(e^+), electron neutrino (υ_e), photon (γ)

$$p + p \rightarrow {}^2D + e^+ + \upsilon_e$$

Timescale ~ 10^{10} years (involves weak interaction so very slow – but there are lots of protons around)

$$p + {}^2D \rightarrow {}^3He + \gamma$$

Timescale ~ 1.4s (strong interaction)

$${}^3He + {}^3He \rightarrow {}^4He + 2p$$

Timescale ~ 10^5 years (strong interaction)

The amount of energy liberated in converting four protons into ^{4}He is 26.2 Mev.

There are two less important side chains to the PP chain known as PPII and PPIII, but these involve more interactions and therefore occur much less frequently. Chapter 4 of "The Physics of Stars" by A.C. Phillips covers thermonuclear fusion in some depth. It is one of these side chains that is responsible for lithium depletion.

III BREMSSTRAHLUNG (BRAKING RADIATION)

Bremsstrahlung is the term used to describe the radiation emitted when a charged particle is scattered when passing through the electric field of the nucleus. A full treatment we require quantum electrodynamics. An approximate derivation is given in section 11.3 of "Nuclear and Particle Physics", by W.S.C Williams (1996).

IV DRAKES EQUATION

It does not require much time to think through the various things that must happen for a star to have a planet in orbit around it which is emitting electromagnetic radiation that we could hope to detect. A radio astronomer called Frank Drake was the first to publish such the resulting equation in 1961.

This equation was put together in order to estimate the number of civilisations in out galaxy from which we come someday hope to contact.

$$N = R \times f_p \times n_e \times f_l \times f_i \times f_c \times L$$

R is the rate at which suitable stars form
f_p is fraction of these stars with which a planetary system has formed
n_e is the number of earth-like planets
f_l is the fraction of these earth-like planets where life develops
f_i is the fraction of these life forms that develop intelligence
f_c is the fraction of intelligent life forms that develop the capability of long distance communications (probably using electromagnetic radiation)
L is the lifetime of the communicating civilizations (i.e. how many years is between development of communications and extinction?)

A particularly pessimistic view on why we have yet to contact any other life forms is that the value of L is very low – i.e. soon after a civilization reaches a state of technological advancement it destroys itself (through nuclear war for example).

V COORDINATES USED FOR OBSERVING

The system of right ascension and declination is analogous to the lines of latitude and longitude on the earth. Declination is measure between 0 and 90 degrees north or south of a plane which intersects the earth through the equator. Right Ascension is measured in units of time, with the equivalent of Greenwich Meridian being the first point of Aries.

Any point on this 'celestial sphere' can therefore be defined by two quantities $-90 < \delta < 90$ and $0h < RA < 24h$. The latter is often converted into degrees by multiplying by 15 so that $0h < RA < 360$

VI DISTANCE MEASUREMENTS

SI units are inconveniently small for use in astrophysics - a more convenient set of units is used.

The *Astronomical Unit* (AU) is the mean distance between the earth and the sun.

$$1AU \approx 10^{11} m .$$

The AU is still inconvenient on scales larger than the solar system (The mean distance of Pluto from the sun is 40 AU). The *Parsec* is defined as the distance at which 1 AU subtends an angle of 1 arcsecond ($1as = \frac{1}{3600}^{\circ}$).

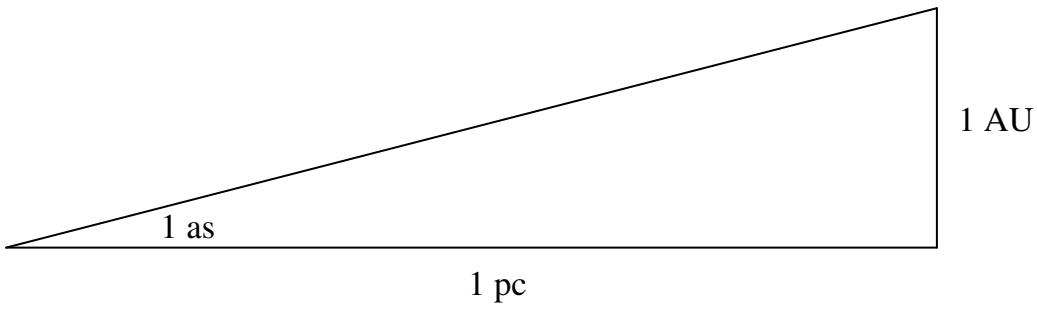

$$1pc = 206265AU$$

Using these units, the nearest star (aside from the sun of course) is ~1pc away, the nearest galaxy to the Milky Way is 670kpc. The radius of the observable universe is ~3000Mpc.

The parsec is preferred over the unit of the light year (the distance light can travel in one year), but for comparison 1pc is about 3.25 light years.

VII THE 14 T TAURI STARS IDENTIFIED IN THIS INVESTIGATION

CTTS – No Coordinates Available (601.66)

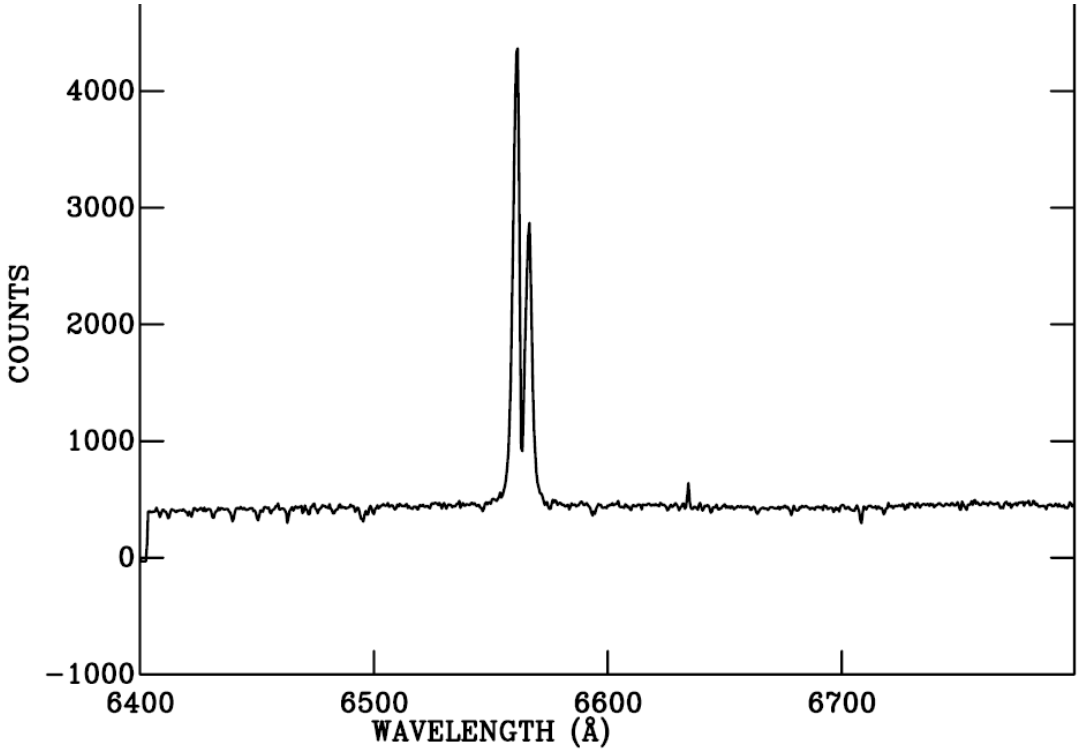

CTTS – No Coordinates Available (601.132)

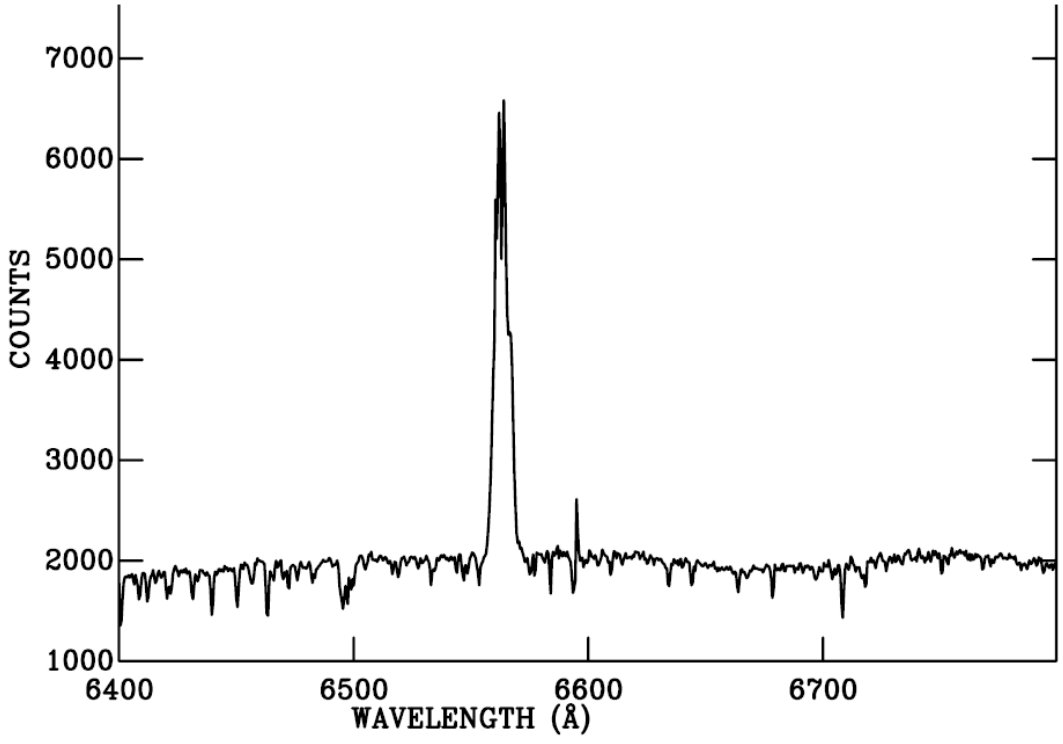

CTTS - 518-89

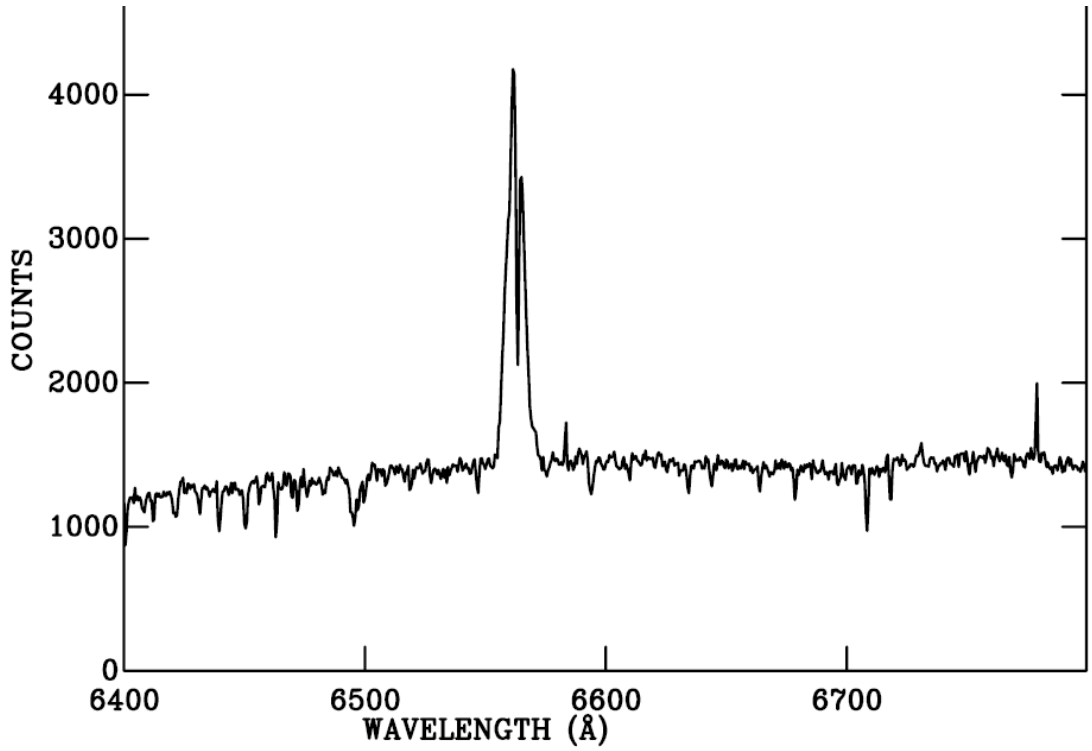

CTTS - 518-148

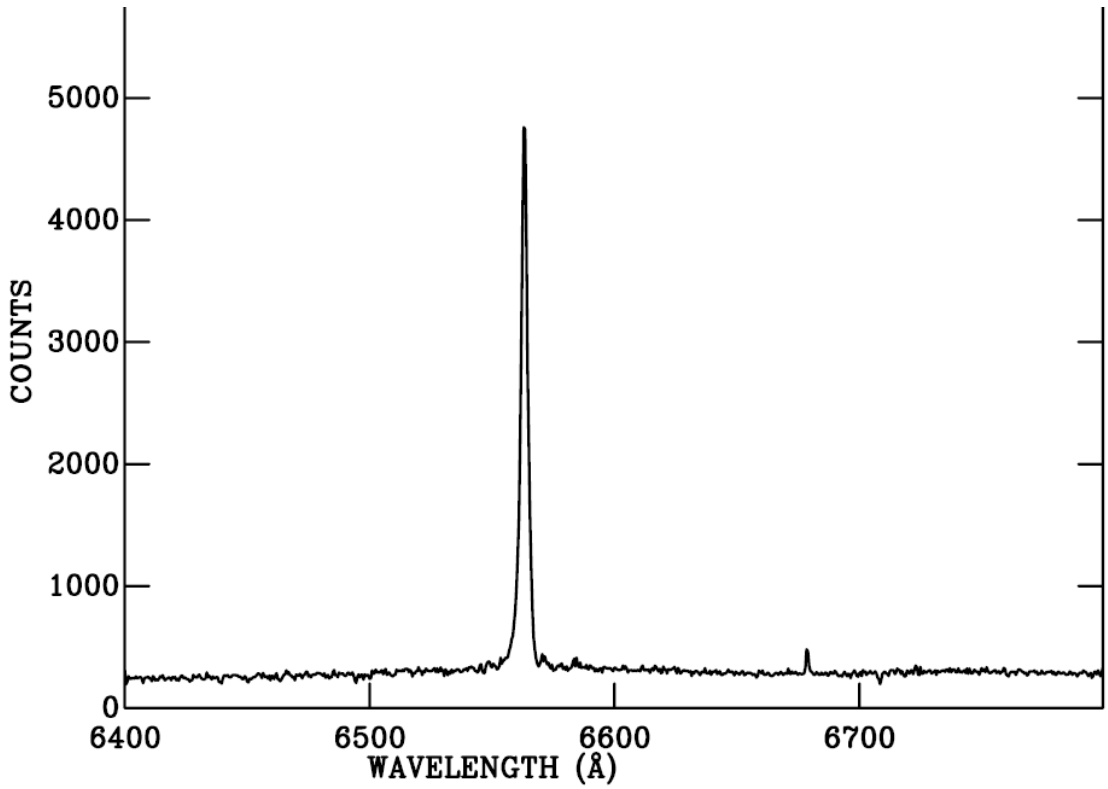

WTTS – Coordinates Not Available (601.26)

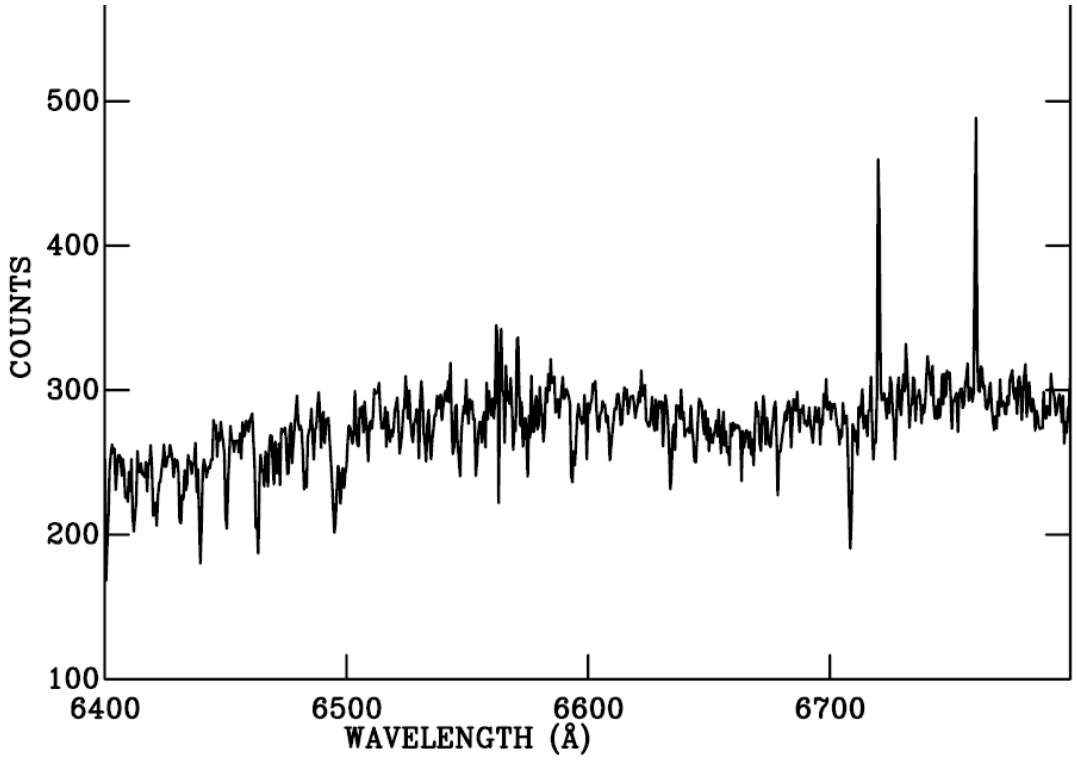

WTTS - 518-40

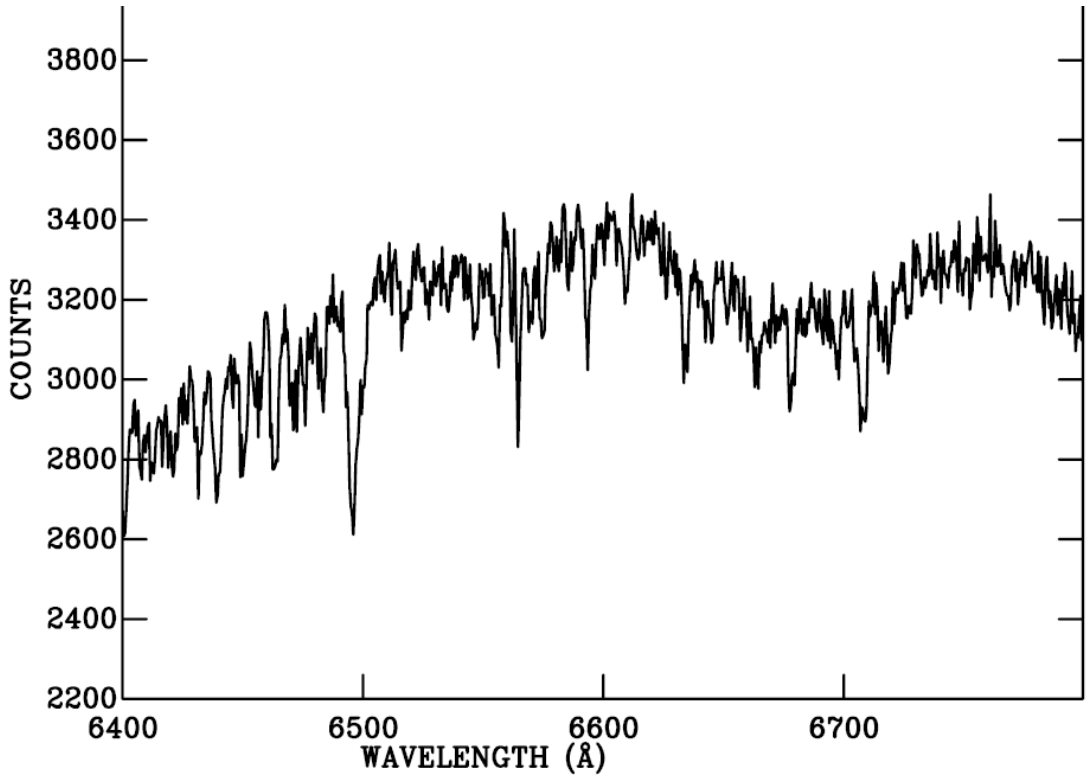

WTTS - 518-59

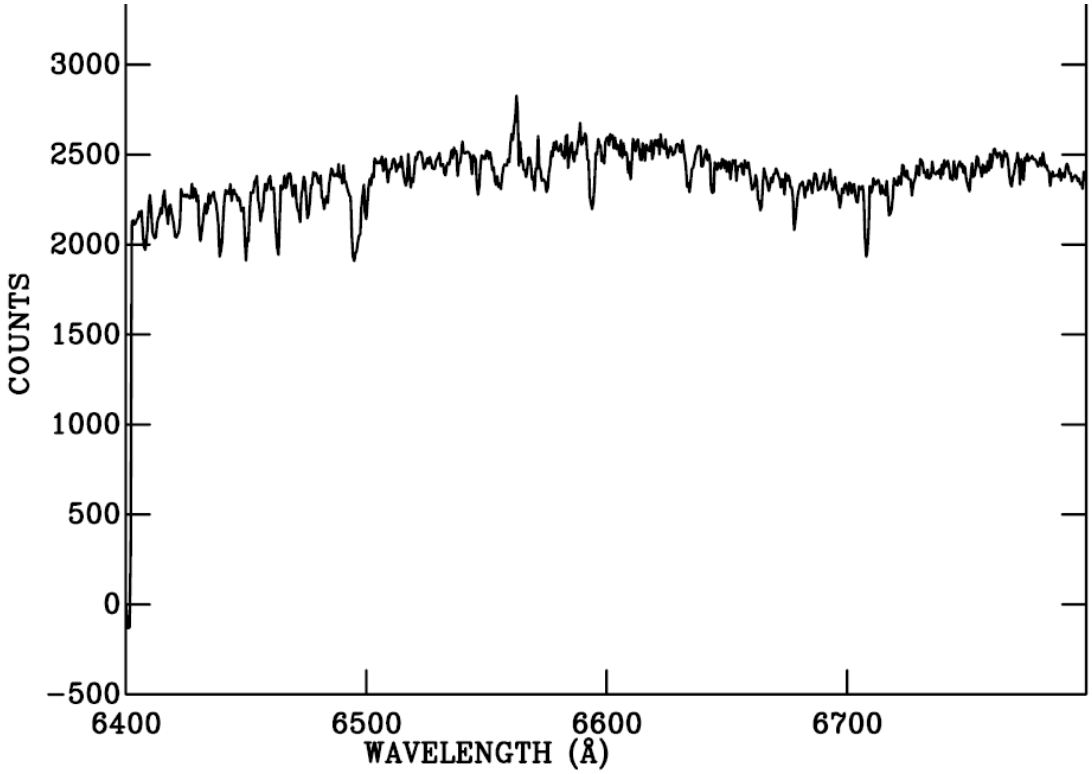

WTTS - 518-91

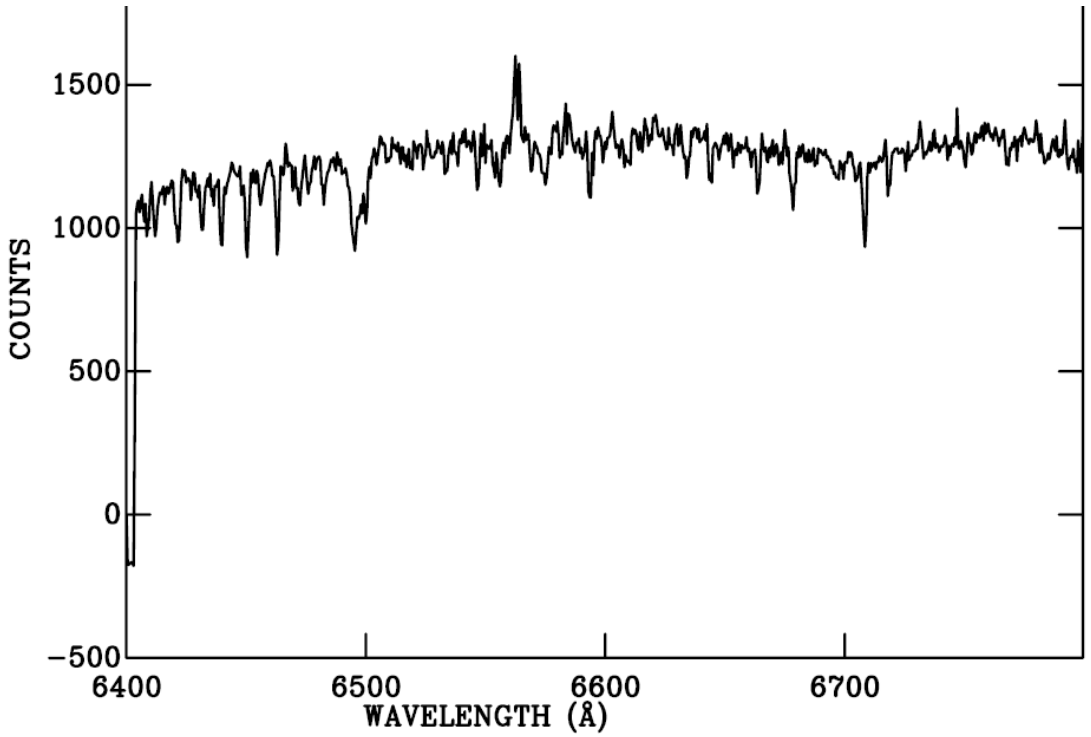

WTTS - 518-105

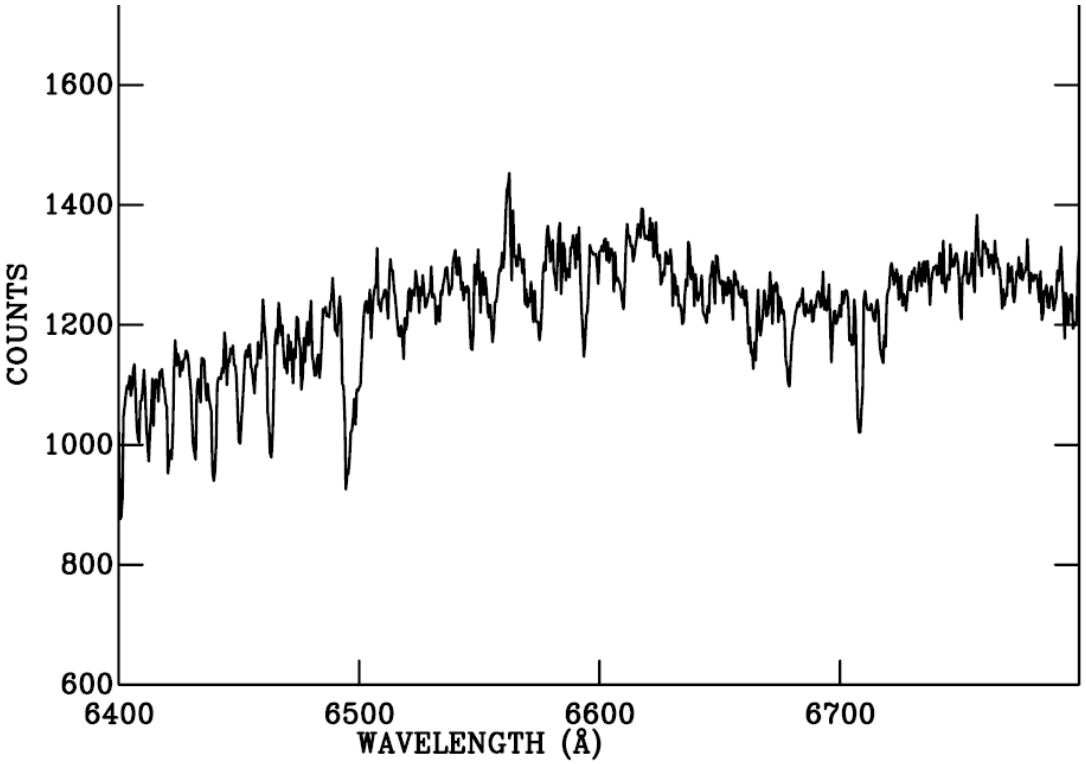

WTTS - 518-109

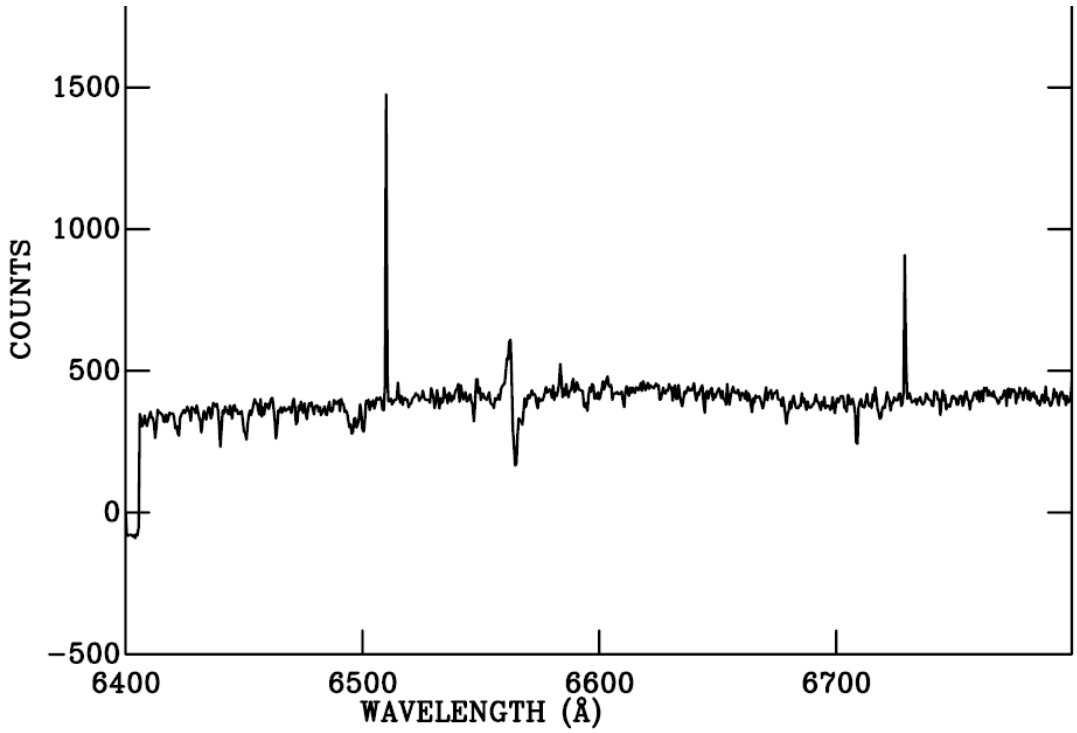

WTTS - 518-123

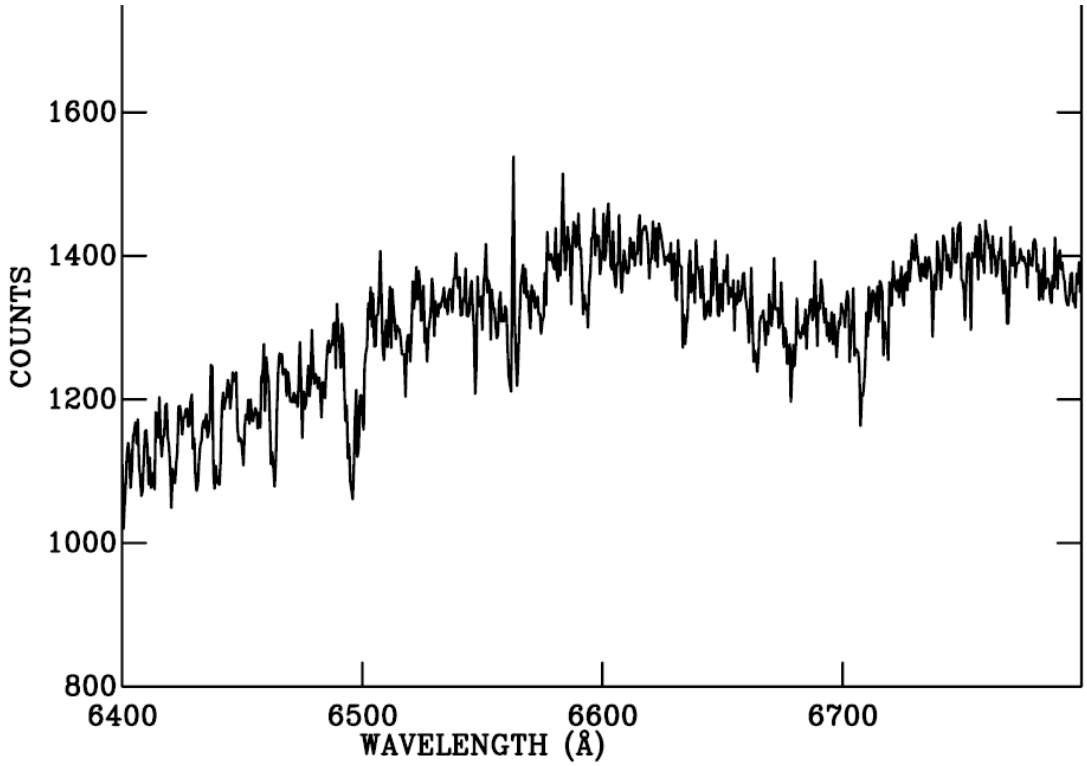

WTTS - 518-135

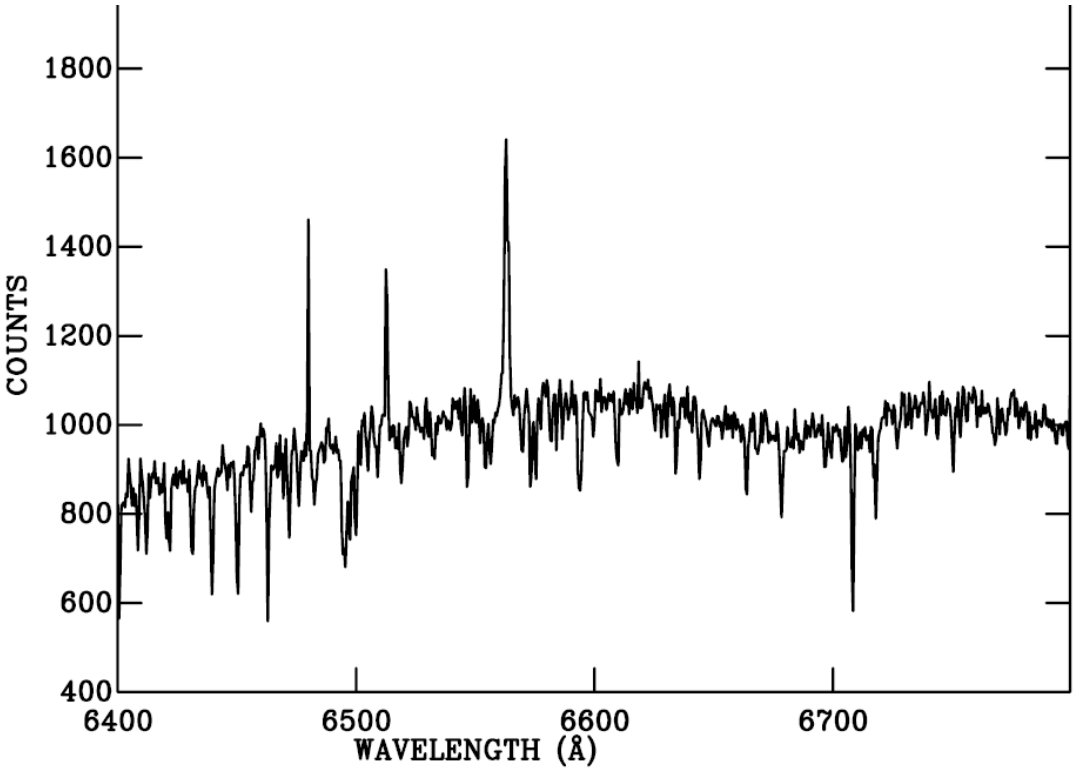

WTTS - 518-138

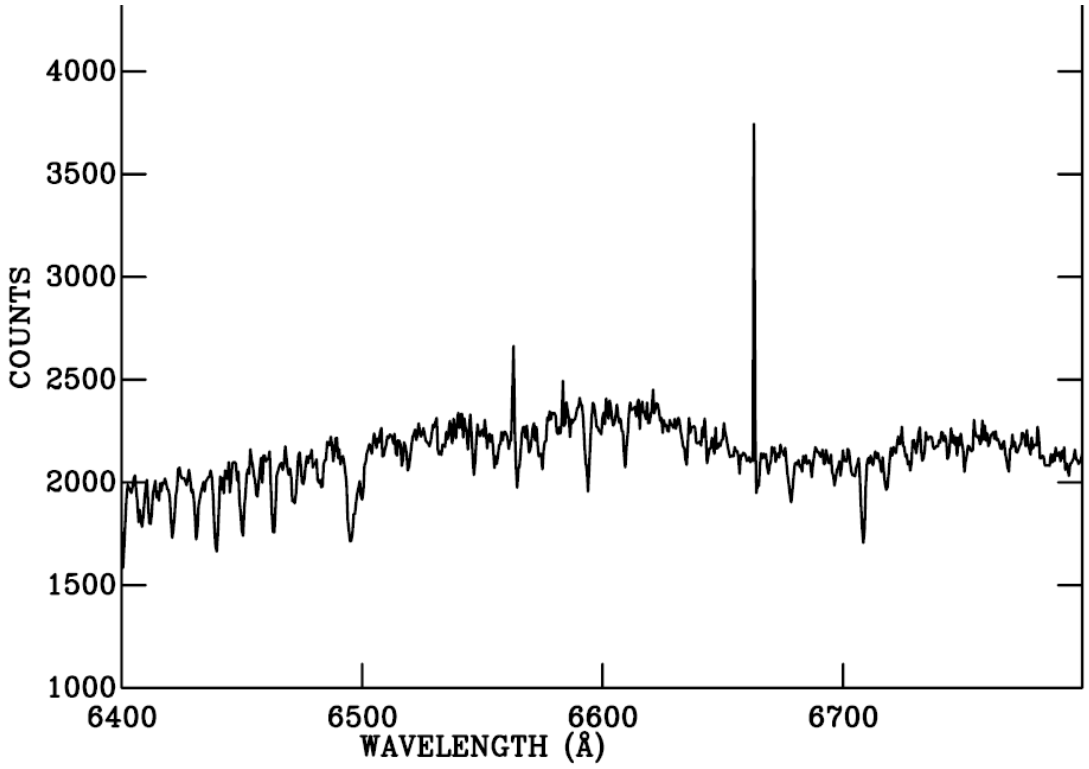

WTTS - 518-151

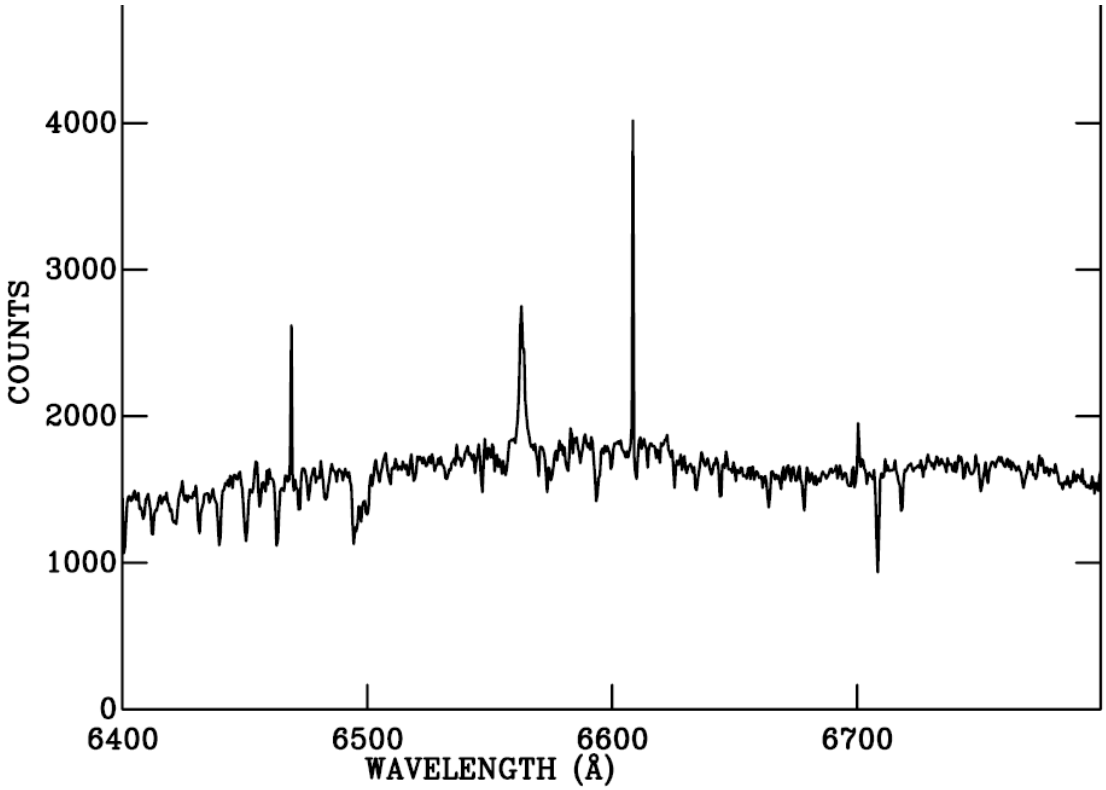

VIII - Hα LINE PROFILES

Three situations fill be discussed - inflows, outflows and rotation.

Inflows (e.g. 518.109 in appendix VII)

Some of the photons emitted by the star are absorbed by the inflowing material, and then re-emitted isotropically, resulting in an absorption line. The absorption line will be red shifted due to the fact that the material is flowing away from us.

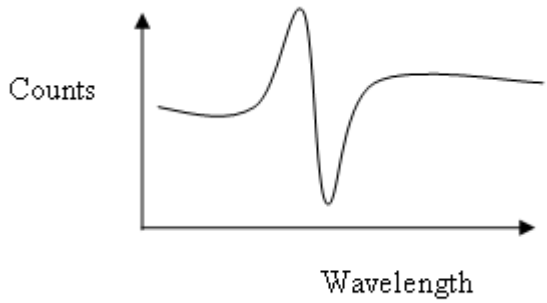

Outflows

The situation is observed, i.e. the absorption line is *blueshifted*.

Rotation

As the star rotates, the receding edge is red shifted and the approaching side is blue shifted, creating a double peak. This example is taken from star 518.89 (See appendix VII)